Simulation-based inference for pulsar-population synthesis

Celsa Pardo Araujo

PhD supervisors: Vanessa Graber and Nanda Rea

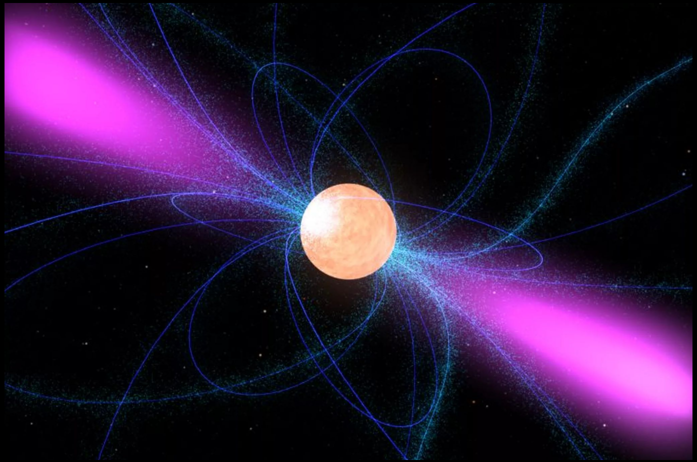

Credits: NASA

pardo@ice.csic.es
graber@ice.csic.es
rea@ice.csic.es
ronchi@ice.csic.es

in collaboration with
Michele Ronchi

MAGNESIA

erc
European Research Council
Established by the European Commission

Institute of Space Sciences
CSIC
Consejo Superior de Investigaciones Científicas
IEEC

EXCELENCIA MARÍA DE MAEZTU

UAB
Universitat Autònoma de Barcelona

Neutron star population

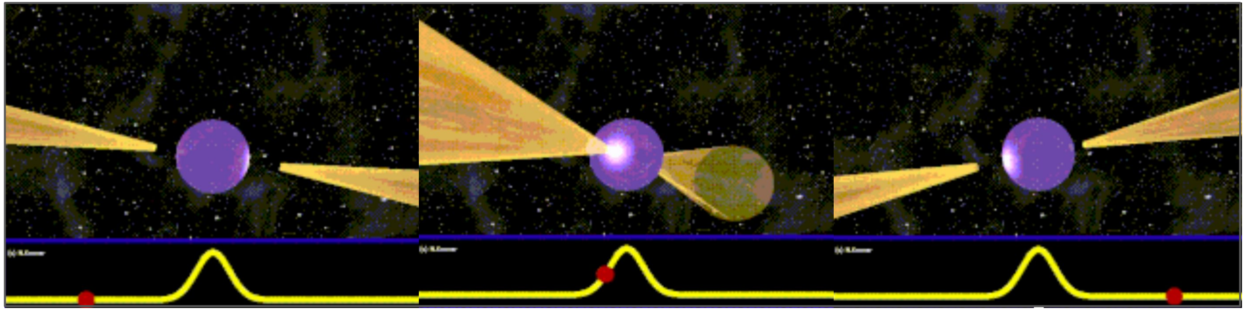

Neutron star population

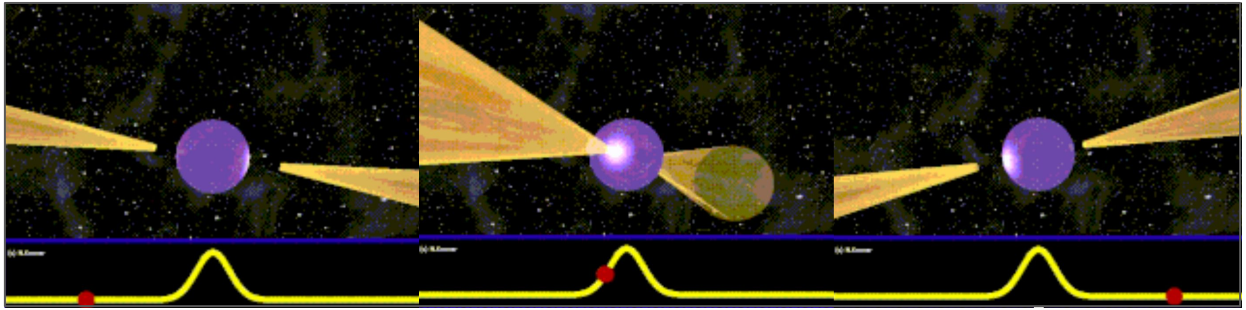

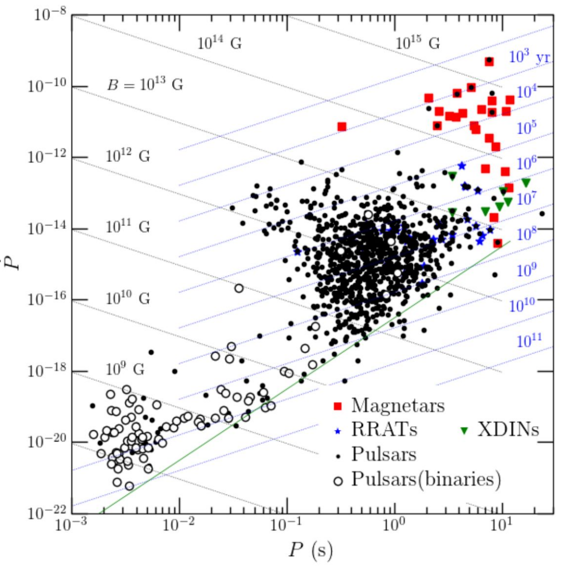

- Different classes of neutron stars occupy different locations in the $P\dot{P}$-plane probing different evolution paths and/or different origins.

Neutron star population

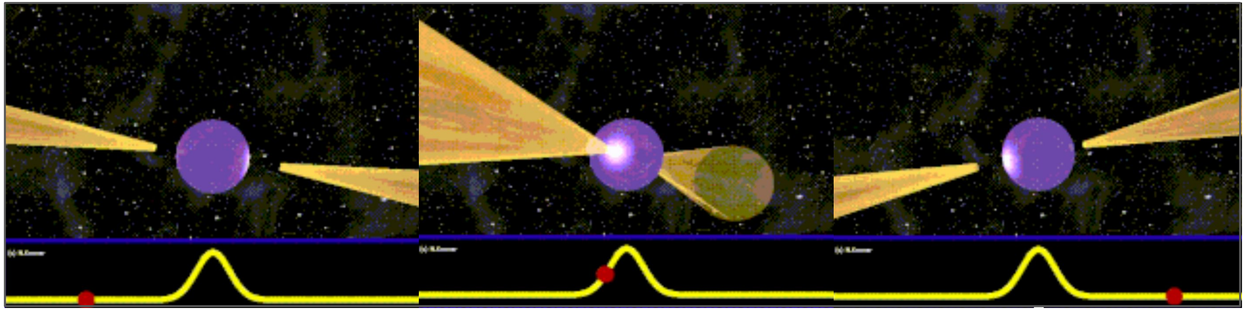

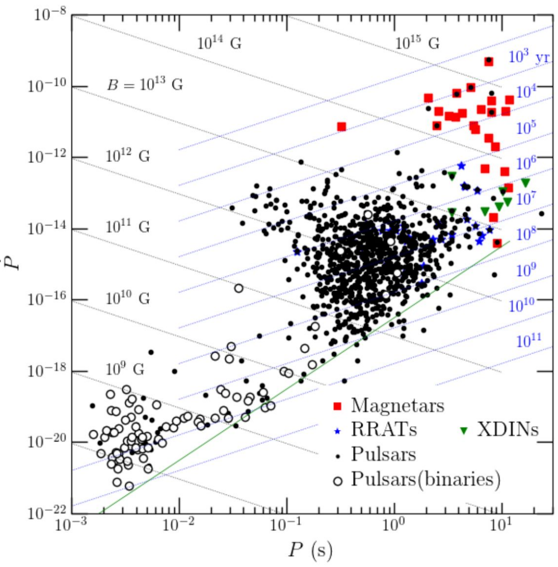

- Different classes of neutron stars occupy different locations in the PṖ-plane probing different evolution paths and/or different origins.

CC supernova rate:
~ 2 per century

×

Galaxy age:
~ 13.6 billion years

=

NS number:
~ 2.8×10^8

Neutron star population

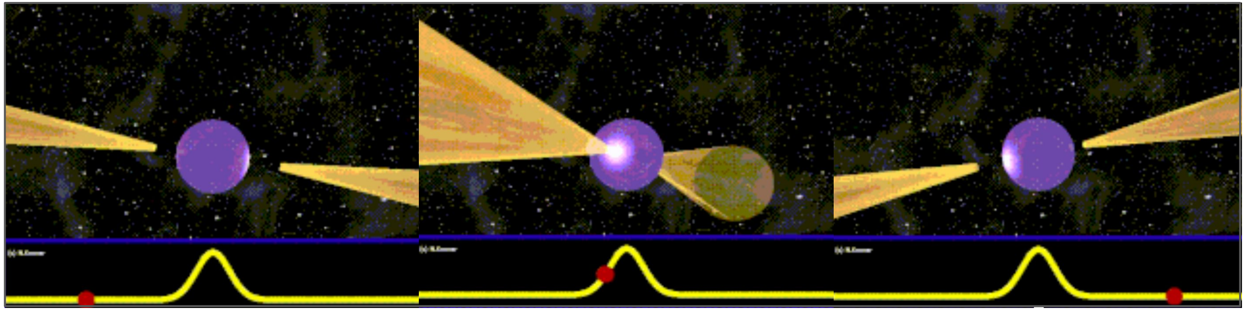

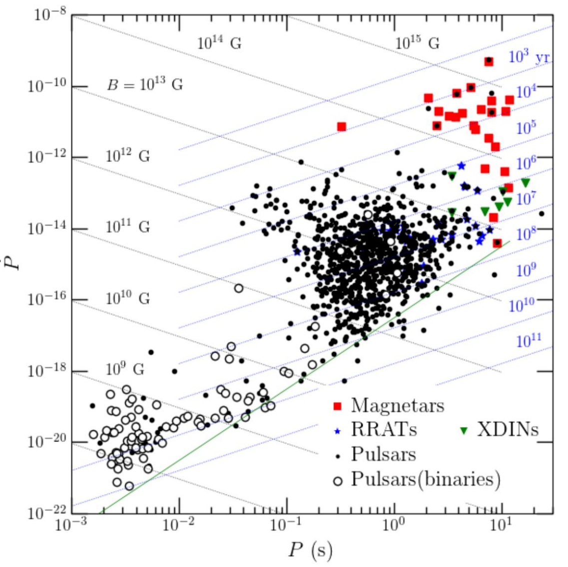

- Different classes of neutron stars occupy different locations in the $P\dot{P}$-plane probing different evolution paths and/or different origins.

CC supernova rate:
~ 2 per century

×

Galaxy age:
~ 13.6 billion years

=

~ 3,000 detected neutron stars!

Population synthesis

- What are the **natal properties** and the **birth rate** of the neutron-star population**?**
- Are there any **evolutionary links between different neutron-star classes?**

Population synthesis

- What are the **natal properties** and the **birth rate** of the neutron-star population?
- Are there any **evolutionary links between different neutron-star classes?**

- Population synthesis focuses on the **entire** population of neutron stars (e.g. Faucher-Giguère & Kaspi 2006, Lorimer et al. 2006, Gullón et al. 2014, Cieślar et al. 2020):

model **birth properties** with Monte-Carlo approach → **evolve properties** forward in time → **apply filters** to mimic observational biases/limits → **compare** mock simulations **to observations** to constrain input

Dynamical evolution

- We evolve the stars' position & velocity by **solving Newtonian equations of motion** in cylindrical galactocentric coordinates: $\ddot{\vec{r}} = -\vec{\nabla}\Phi_{\rm MW}$

Top view

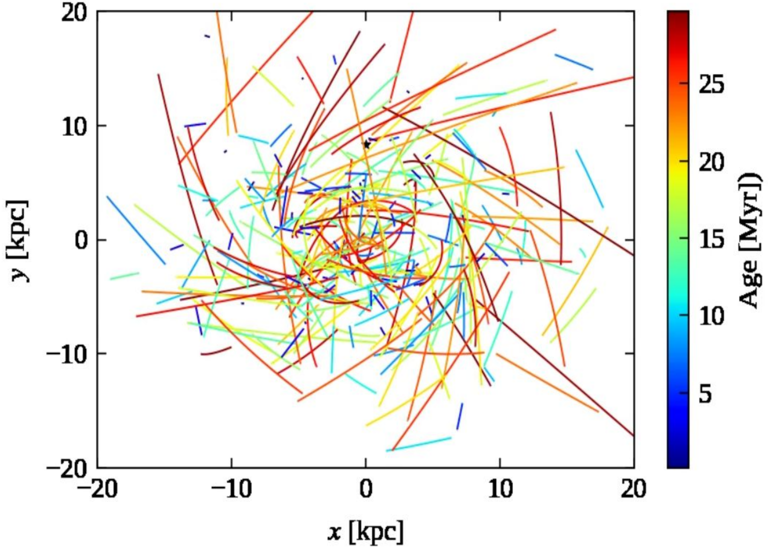

Side view

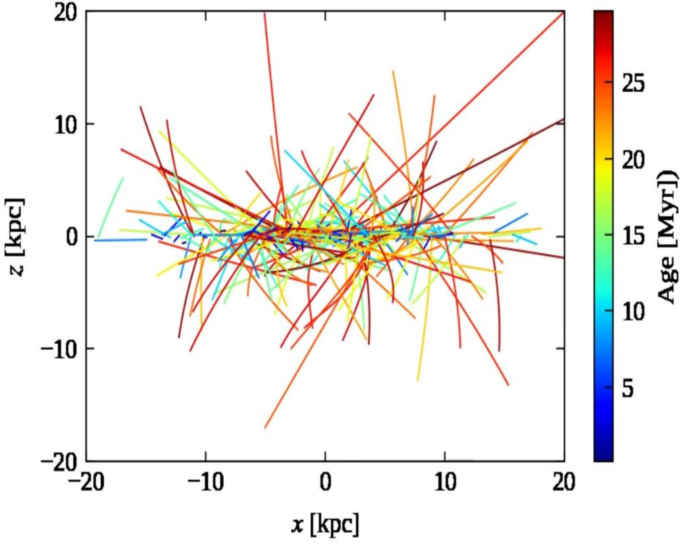

Magneto-rotational evolution

- The neutron-star magnetosphere exerts a **torque onto the star**. This causes **spin-down** and **alignment of the magnetic and rotation axes** (Spitkovsky 2006, Philippov et al. 2014).

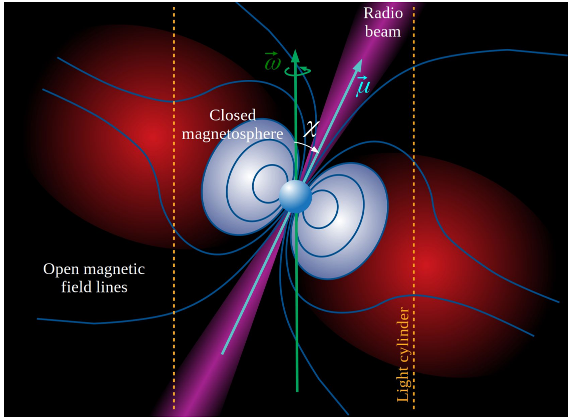

- The neutron-star magnetosphere exerts a **torque onto the star**. This causes **spin-down** and **alignment of the magnetic and rotation axes** (Spitkovsky 2006, Philippov et al. 2014).

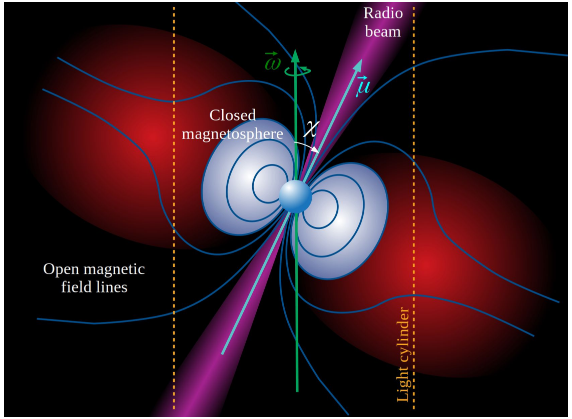

- Neutron star **magnetic fields decay** due to the Hall effect and Ohmic dissipation in the outer stellar layer (crust) (e.g., Viganó et al. 2013 & 2021, Gourgouliatos et al. 2014, De Grandis et al. 2020).

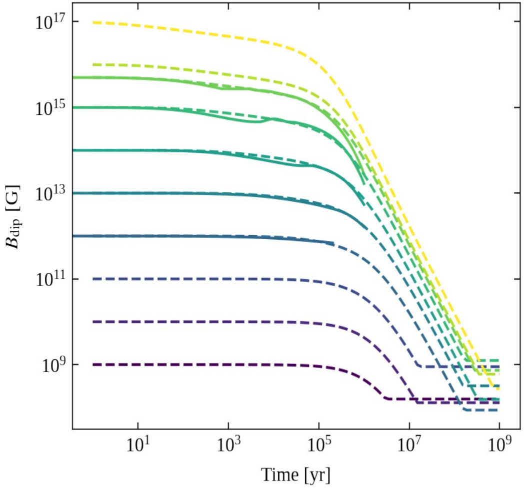

Radio surveys:

- **Parkes Multibeam Pulsar Survey** (PMPS)
- **Swinburne Parkes Multibeam Pulsar Survey** (SMPS)
- **High Time Resolution Universe Survey** (HTRU)

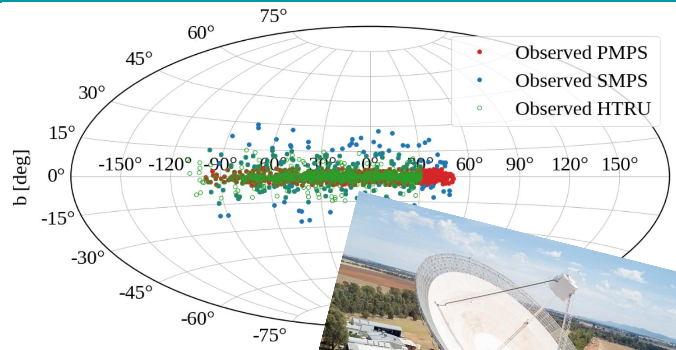

Radio surveys & Goals

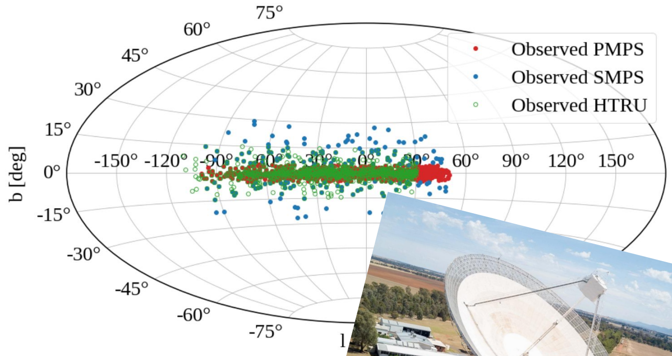

Radio surveys:

- **Parkes Multibeam Pulsar Survey** (PMPS)
- **Swinburne Parkes Multibeam Pulsar Survey** (SMPS)
- **High Time Resolution Universe Survey** (HTRU)

We want to infer:

- Period distribution at birth.
- Magnetic field distribution at birth.

Assumptions

- **Initial periods** follow a normal in log with $\mu_{\log P}$ and $\sigma_{\log P}$ (Igoshev et al. 2022)
- **Initial fields** follow a normal in log with $\mu_{\log B}$ and $\sigma_{\log B}$ (Gullón et al. 2014)

Simulation based inference

1. **sample** θ_i from the prior $\pi(\theta)$, for $i = 1, \ldots, N$

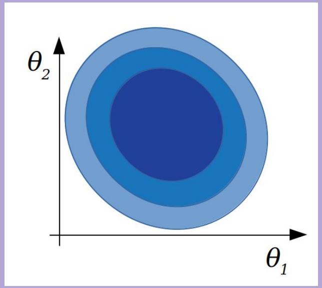

2. **run simulator** for θ_i to produce mock observations: $x_i \sim P(x|\theta_i)$

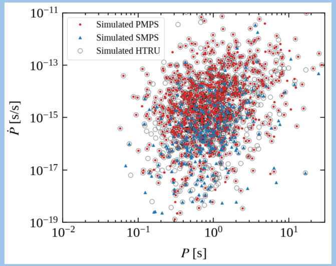

3. Generate the **training dataset:**

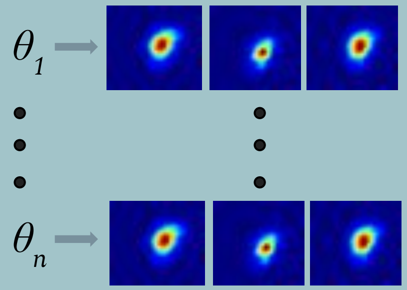

neural network (conditional density estimator) on simulated data to approximate the posterior

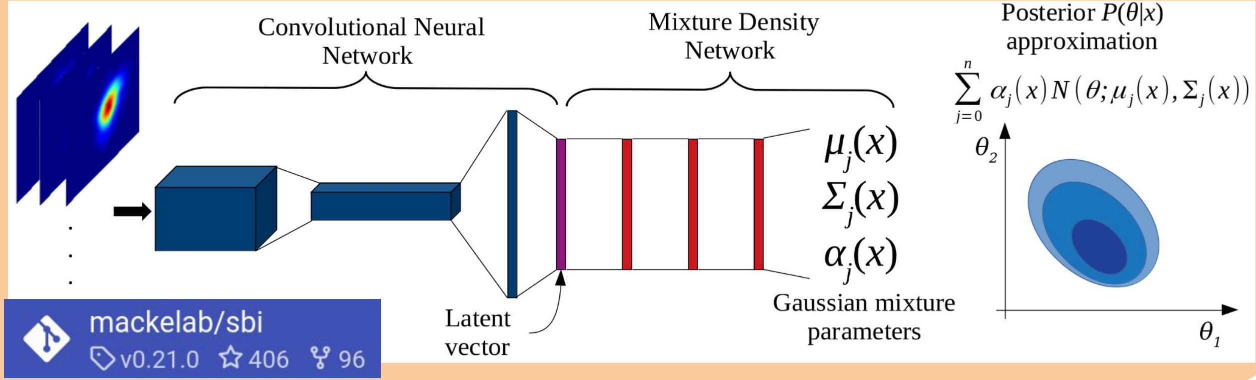

Results

- 360,000 simulations in total, we use 80 % for training, 10 % for validation, 10 % for testing.

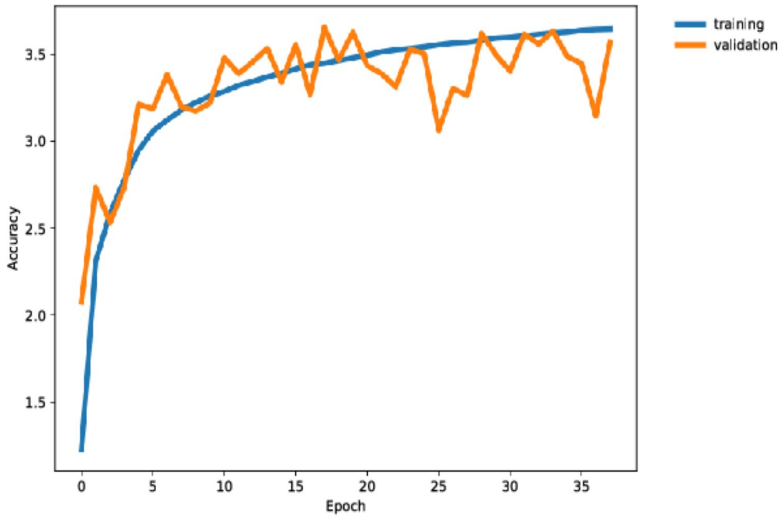

Results

- 360,000 simulations in total, we use 80 % for training, 10 % for validation, 10 % for testing.

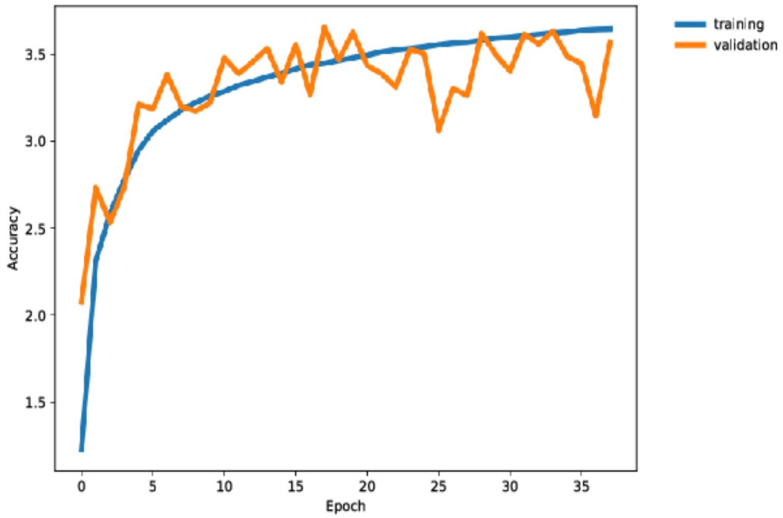

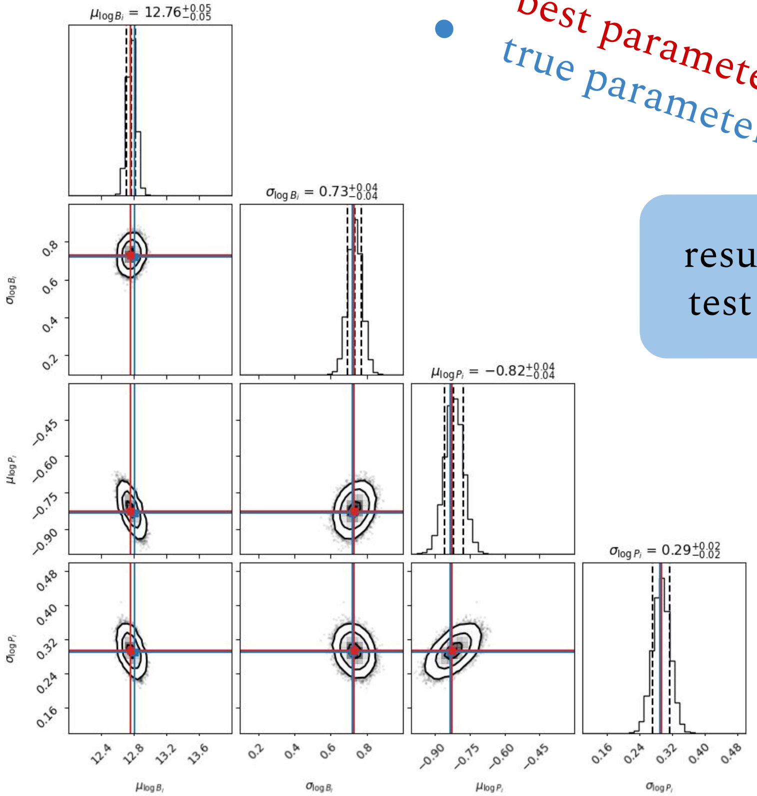

best parameters

true parameters

results for a test sample

Results for the observed population

With our optimised neural network, we can also **infer the posteriors** for the **pulsar population detected in our three surveys** and recover the following constraints:

$$\mu_{\log B} = 13.07^{+0.07}_{-0.08}$$

$$\sigma_{\log B} = 0.43^{+0.03}_{-0.03}$$

$$\mu_{\log P} = -0.98^{+0.25}_{-0.29}$$

$$\sigma_{\log P} = 0.54^{+0.33}_{-0.25}$$

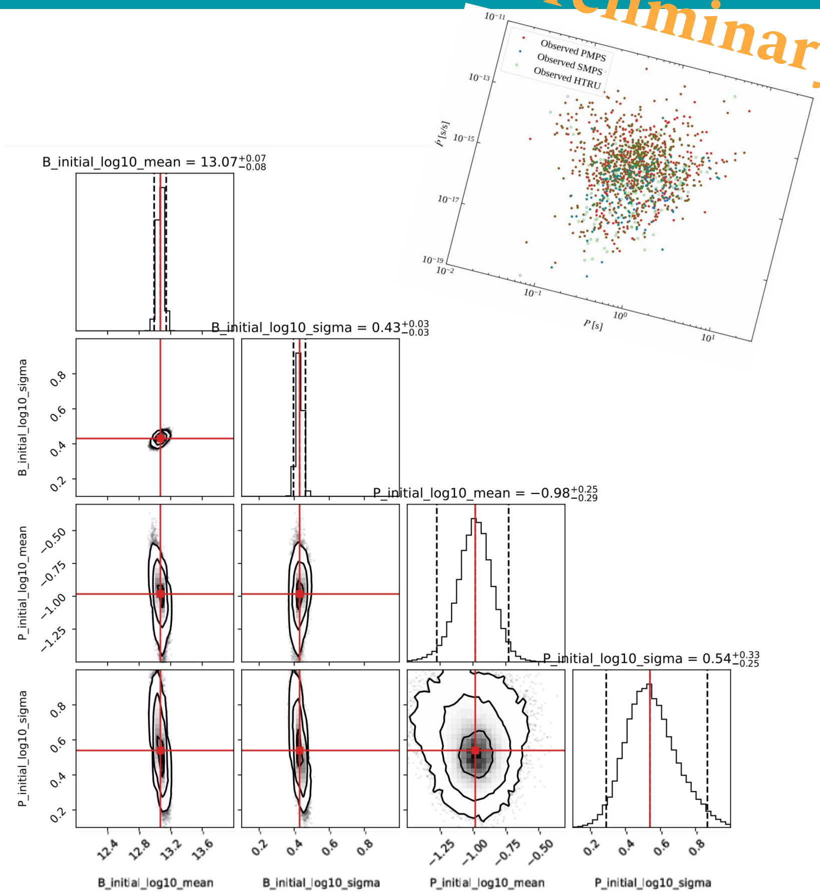

Thanks for listening!

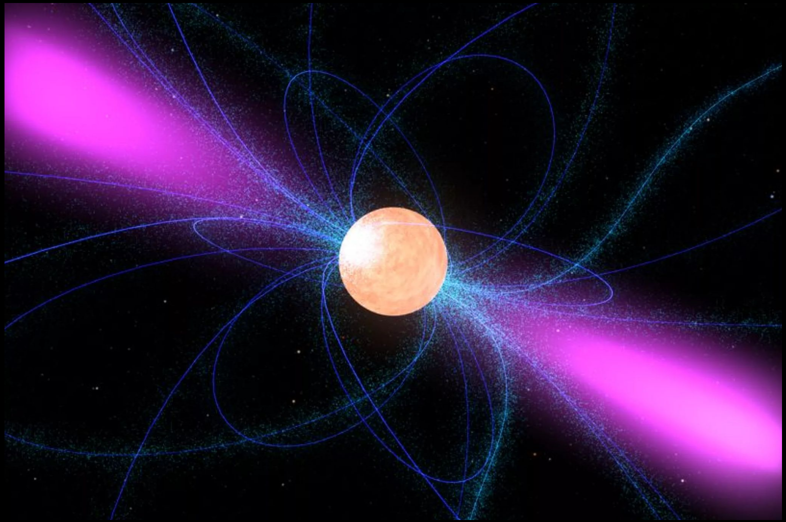

Credits: NASA

MAGNESIA

erc
European Research Council
Established by the European Commission

Institute of Space Sciences

CSIC IEEC
Consejo Superior de Investigaciones Científicas

EXCELENCIA
MARÍA
DE MAEZTU

UAB
Universitat Autònoma de Barcelona

Radio surveys

- We compare our simulated populations with three surveys from Murriyang (the Parkes Radio Telescope):
  - **Parkes Multibeam Pulsar Survey** (PMPS) (Manchester et al. 2001, Lorimer et al. 2006): *1,009 isolated pulsars*
  - **Swinburne Parkes Multibeam Pulsar Survey** (SMPS) (Edwards et al. 2001, Jacoby et al. 2009): *218 isolated pulsars*
  - **High Time Resolution Universe Survey** (HTRU) (Keith et al. 2018): *1,023 isolated pulsars*

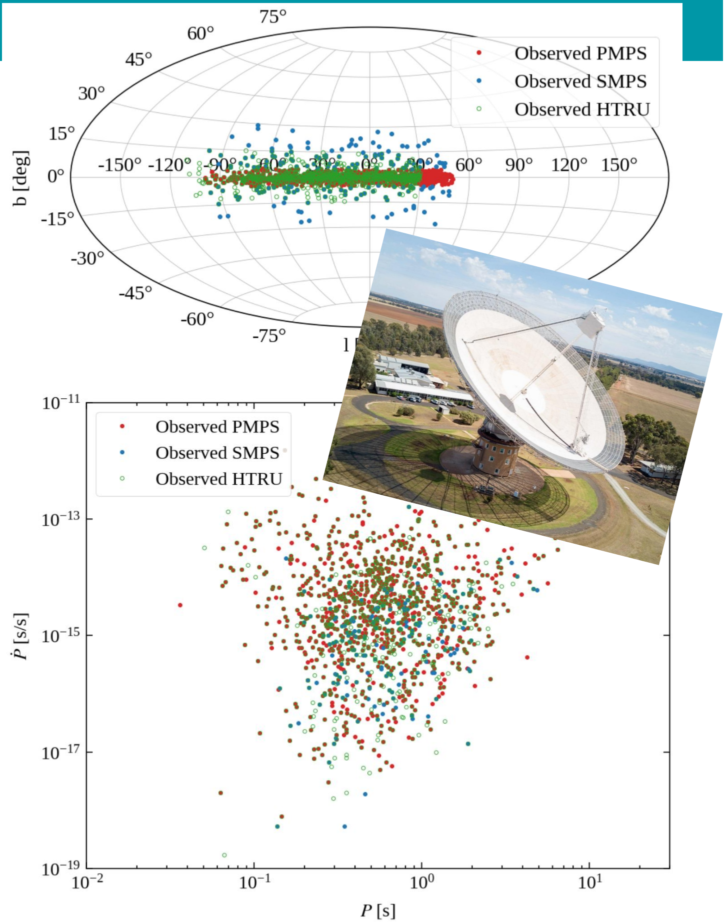

Radio emission and detection

- The stars' **rotational energy E_{rot}** is converted into coherent radio emission (Faucher-Giguère & Kaspi 2006; Gullón et al. 2014).

$$L_{\rm radio} = L_0 \left(\frac{\dot{P}}{P^3} \right)^{1/2} \propto \dot{E}_{\rm rot}^{1/2}$$

- As **emission is beamed**, ~ 90% of pulsars do not point towards us. For those intercepting our line of sight, compute **radio flux S_{radio}** & **pulse width W**.

$$S_{\rm radio} = \frac{L_{\rm radio}}{\Omega_{\rm beam} d^2}$$

- A **signal-to-noise ratio** can be estimated through the **radiometer equation**.

$$S/N = \frac{S_{\rm mean} G \sqrt{N_{\rm pol} \Delta\nu \Delta t_{\rm obs}}}{\beta \left(T_{\rm rec} + T_{\rm sky}(l,b) \right)} \sqrt{\frac{P - w_{\rm eff}}{w_{\rm eff}}}$$

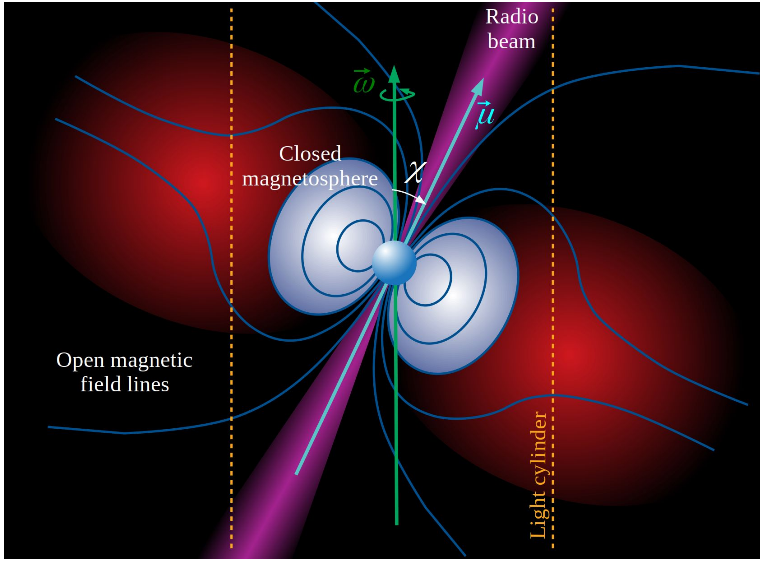

A pulsar counts as detected, if it **exceeds the sensitivity threshold** for a survey recorded with a specific radio telescope.

Magneto-rotational evolution

$$\dot{P} = \frac{\pi^2}{c^3}\frac{B^2 R^6}{IP}\left(\kappa_0 + \kappa_1 \sin^2\chi\right)$$

$$\dot{\chi} = -\frac{\pi^2}{c^3}\frac{B^2 R^6}{IP^2}\left(\kappa_2 \sin\chi \cos\chi\right)$$

(Spitkovsky 2006, Philippov et al. 2014)

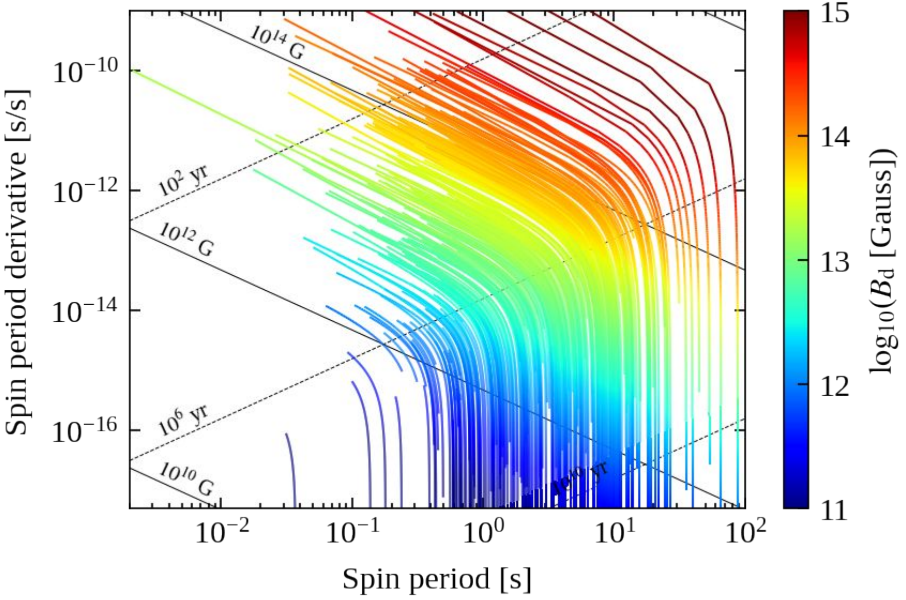

$P\dot{P}$ evolution tracks for

$\mu_{\log P}$ = -0.6 , $\sigma_{\log P}$ = 0.3 , $\mu_{\log B}$ = 13.25, $\sigma_{\log B}$ = 0.75 and α = *-2.0*